Antiviral Research 172 (2019) 104641

Contents lists available at ScienceDirect

Antiviral Research

journal homepage: www.elsevier.com/locate/antiviral

Reevaluation of the efficacy of favipiravir against rabies virus using *in vivo* imaging analysis

Kentaro Yamada[a], Kazuko Noguchi[b,c,1], Kazunori Kimitsuki[b], Ryo Kaimori[b], Nobuo Saito[b], Takashi Komeno[d], Nozomi Nakajima[d], Yousuke Furuta[d], Akira Nishizono[a,b,*]

[a] Research Promotion Institute, Faculty of Medicine, Oita University, 1-1 Idaigaoka, Hasama-machi, Yufu City, Oita, 879-5593, Japan
[b] Department of Microbiology, Faculty of Medicine, Oita University, 1-1 Idaigaoka, Hasama-machi, Yufu City, Oita, 879-5593, Japan
[c] Department of Food Science and Technology, Minami Kyushu University, 5-1-2 Kirishima, Miyazaki City, Miyazaki, 880-0031, Japan
[d] FUJIFILM Toyama Chemical Co.,Ltd, 2-4-1 Shimookui, Toyama City, Toyama, 930-8508, Japan

ARTICLE INFO

Keywords:
Rabies virus
Favipiravir
Red firefly luciferase
In vivo bioluminescence imaging

ABSTRACT

Rabies virus (RABV) is a highly neurotropic virus and the causative agent of rabies, an encephalitis with an almost 100% case-fatality rate that remains incurable after the onset of symptoms. Favipiravir (T-705), a broad-spectrum antiviral drug against RNA viruses, has been shown to be effective against RABV *in vitro* but ineffective *in vivo*. We hypothesized that favipiravir is effective in infected mice when RABV replicates in the peripheral tissues/nerves but not after virus neuroinvasion. We attempted to clarify this point in this study using *in vivo* bioluminescence imaging. We generated a recombinant RABV from the field isolate 1088, which expressed red firefly luciferase (1088/RFLuc). This allowed semiquantitative detection and monitoring of primary replication at the inoculation site and viral spread in the central nervous system (CNS) in the same mice. Bioluminescence imaging revealed that favipiravir (300 mg/kg/day) treatment commencing 1 h after intramuscular inoculation of RABV efficiently suppressed viral replication at the inoculation site and the subsequent replication in the CNS. However, virus replication in the CNS was not inhibited when the treatment began 2 days after inoculation. We also found that higher doses (600 or 900 mg/kg/day) of favipiravir could suppress viral replication in the CNS even when administration started 2 days after inoculation. These results support our hypothesis and suggest that a highly effective drug-delivery system into the CNS and/or the enhancement of favipiravir conversion to its active form are required to improve favipiravir treatment of rabies. Furthermore, the bioluminescence imaging system established in this study will facilitate the development of treatment for symptomatic rabies.

1. Introduction

Rabies virus (RABV) belongs to the genus Lyssavirus, family Rhabdoviridae of the order Mononegavirales, *which is a group of* viruses with a negative-sense, single-stranded RNA genome. RABV is the causative agent of rabies, which is an acute encephalitis with a case-fatality rate of almost 100% that kills approximately 59,000 people annually worldwide (Hampson et al., 2015). RABV is generally transmitted by the bite of an infected animal. RABV enters peripheral nerves at the sites of infection and then disseminates and replicates in the central nervous system (CNS), resulting in the appearance of symptoms (Fooks et al., 2017). Although the development of rabies symptoms is preventable when postexposure prophylaxis, a series of repeated vaccinations, is correctly administered during the incubation period (usually 30–90 days), there is still no effective cure for rabies after the onset of symptoms.

Several attempts to develop a therapy for rabies have been reported (Banyard et al., 2019; Dufkova et al., 2019; Koraka et al., 2019; Marosi et al., 2019; Martina et al., 2019; Mechlia et al., 2019; Rogee et al., 2019; Smreczak et al., 2019; Virojanapirom et al., 2016; Yamada et al.,

Abbreviations: BBB, blood–brain barrier; BSCB, blood–spinal cord barrier; CCD, charge-coupled device; CI, confidence interval; CNS, central nervous system; dpi, days postinoculation; EM, electron multiplying; EMG, electron-multiplying gain; EXP, exposure time; FCS, fetal calf serum; FFU, focus-forming units; FLuc, firefly luciferase; hpi, h postinoculation; HPRT, hypoxanthine-guanine phosphoribosyltransferase; IC_{50}, half-maximal inhibitory concentration; i.p., intraperitoneally; MEM, Eagle's minimal essential medium; MOI, multiplicity of infection; PBS, phosphate-buffered saline; RABV, rabies virus; RFLuc, red firefly luciferase; RIG, rabies immunoglobulin; ROI, region of interest; RLU, relative light unit; WT, wild type

* Corresponding author. Department of Microbiology, Faculty of Medicine, Oita University, 1-1 Idaigaoka, Hasama-machi, Yufu city, Oita, 879-5593, Japan.
E-mail address: a24zono@oita-u.ac.jp (A. Nishizono).
[1] Present address: Oita University Institute of Advanced Medicine, Inc., 17–20 Higashikasuga-machi, Oita city, Oita, 870–0037, Japan.

https://doi.org/10.1016/j.antiviral.2019.104641
Received 6 August 2019; Received in revised form 13 October 2019; Accepted 23 October 2019
Available online 28 October 2019

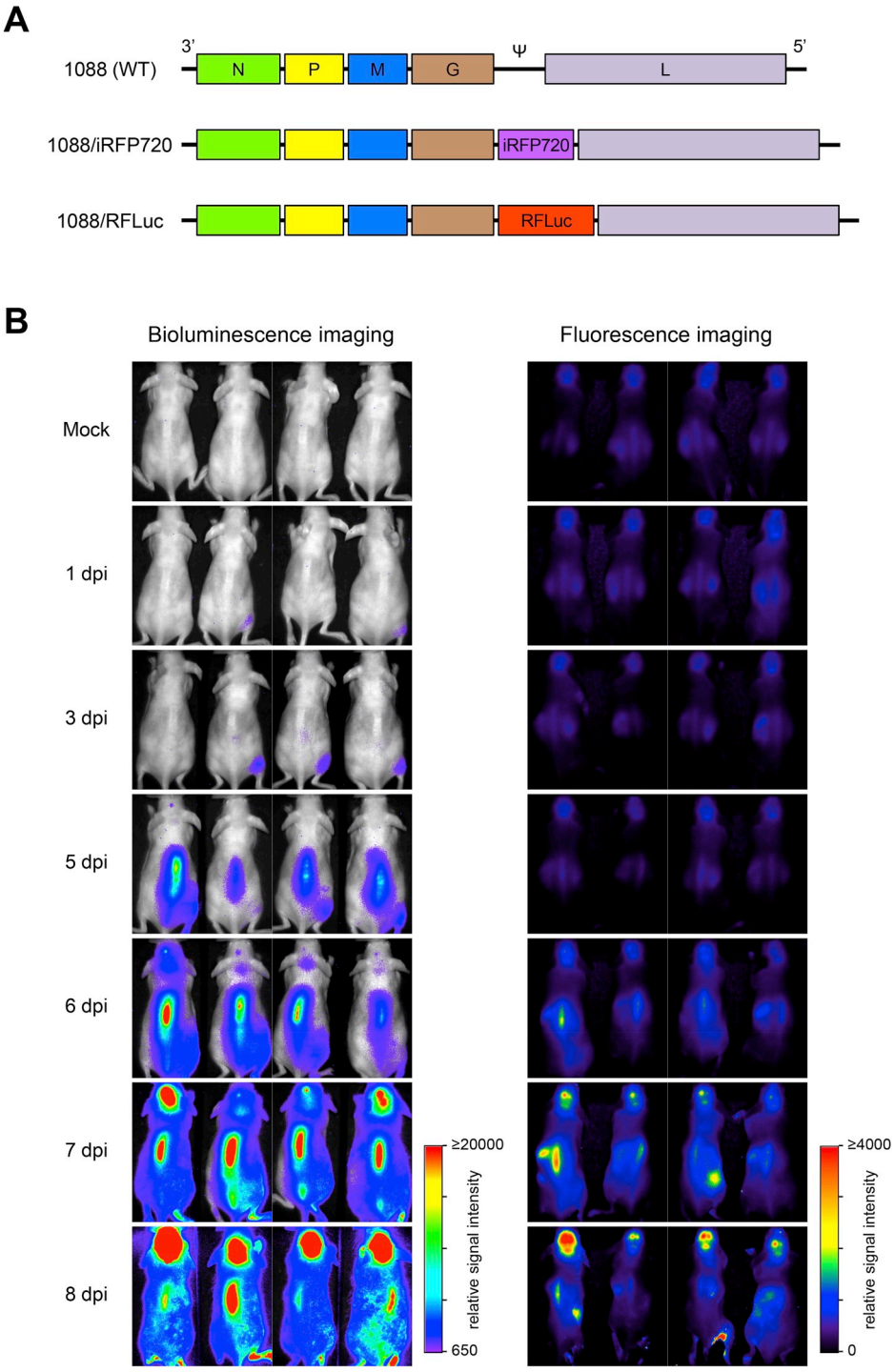

Fig. 1. (A) Schematic diagram of genome structure of recombinant RABVs (the 1088 strain) used in this study. The expression cassette for iRFP720 or RFLuc was inserted into the G–L noncoding, pseudogene (Ψ), region of the recombinant virus genome. N, P, M, G, and L indicate nucleoprotein, phosphoprotein, matrix protein, glycoprotein, and large protein genes, respectively. (B) *In vivo* bioluminescence or fluorescence imaging of mice infected with 1088/RFLuc or 1088/iRFP720, respectively. Groups of four hairless mice (Hos:HR-1) were inoculated with each virus (5×10^5 FFU) in the right hindlimb muscle. Then, bioluminescence or fluorescence images were obtained daily using the Lumazone imaging system. The 1088/RFLuc-inoculated mice were administered D-luciferin (150 mg/kg, i.p.) before bioluminescence imaging. Pseudocolor bioluminescence images merged with bright-field images are shown. Fluorescence images of 1088/iRFP720-inoculated mice were obtained using the filter set, 710/40 nm for excitation and 785/62 nm for emission, and shown are as pseudocolor images. The scale bars indicate relative signal intensity.

2016), but with limited success. We have also examined the efficacy of favipiravir (6-fluoro-3-hydroxy-2-pyrazinecarboxamide) against RABV infection in a mouse model (Yamada et al., 2016). Favipiravir, also known as T-705, is a purine analog that has been shown to be active against a broad range of RNA viruses by acting as a chain terminator or mutagen for the viral RNA-dependent RNA polymerase (Furuta et al., 2013). In our study, we showed that favipiravir was effective when administration commenced 1 h after inoculation but ineffective if administered 2 days or more after inoculation (Yamada et al., 2016). Hence, we hypothesized that because the blood–brain barrier (BBB) and blood–spinal cord barrier (BSCB) are known to limit drug delivery into the CNS, favipiravir might be ineffective after virus invasion of the CNS. To clarify when, where, and how drugs work *in vivo* is important for the development of an effective treatment for rabies.

In vivo imaging is a noninvasive method that allows tracking of real-time quantitative temporospatial data for virus replication over time in individual animals (Mehle, 2015). This method has been shown to be useful for evaluation of the efficacy of antiviral drugs in small animals (Fuentes et al., 2017; Guo et al., 2014; Hwang et al., 2008; Luker et al., 2002; Rameix-Welti et al., 2014; Tran et al., 2015). Recently, we

showed that the near-infrared fluorescent protein iRFP720 (Shcherbakova and Verkhusha, 2013) is suitable for *in vivo* fluorescence imaging of RABV infection (Isomura et al., 2017). Using the RABV strain 1088, which is a highly neuroinvasive field isolate (street virus) (Mifune et al., 1979; Yamada et al., 2012), we generated a recombinant RABV expressing iRFP720 (1088/iRFP720). The replication dynamics of RABV were tracked in mice infected with 1088/iRFP720; however, this imaging system exhibited a limited ability to detect the early infection phase because of autofluorescence, suggesting that a more-sensitive method is needed to test the hypothesis stated above. Bioluminescence imaging has a better signal-to-noise ratio because there is little background luminescence (Troy et al., 2004), although substrate injection and an ultrasensitive camera are required. Although firefly luciferase (FLuc), which emits yellow–green light with a peak around 560 nm, is widely used for the live imaging of viral infection (Mehle, 2015), red-shifted FLuc, which is a mutant FLuc with an emission peak at > 600 nm, is more suitable for the *in vivo* imaging of pathogen infection compared with the wild-type (WT) FLuc (Dorsaz et al., 2017; McLatchie et al., 2013). In fact, tissue transparency is higher at longer wavelengths (> 600 nm) than it is in the wavelength range of 500–600 nm (Hong et al., 2017; Rice et al., 2001).

In the present study, we established a method for *in vivo* bioluminescence imaging of RABV infection using the red-shifted FLuc. This approach enabled the highly sensitive monitoring of RABV replication dynamics in mice. Furthermore, we succeeded in using this system to monitor how favipiravir impacted RABV replication in mice.

2. Materials and methods

2.1. Compound

Favipiravir was synthesized at FUJIFILM Toyama Chemical Co., Ltd. (Toyama, Japan) and prepared as described previously (Yamada et al., 2016). For cell culture-based experiments, favipiravir was dissolved in Eagle's minimal essential medium (MEM) as a 10 mM stock solution. For animal experiments, favipiravir was suspended in 0.5% methylcellulose (viscosity, 400 cP; Sigma-Aldrich). The favipiravir solutions were stored at 4 °C and used within 1 week.

2.2. Viruses and cells

Mouse neuroblastoma cell lines, Neuro-2a cells and NA cells, and human neuroblastoma cell line SK-N-SH cells were maintained in MEM supplemented with 10% fetal calf serum (FCS). BHK cells that stably express T7 RNA polymerase (BHK/T7-9 cells) (Ito et al., 2003) were maintained in MEM supplemented with 5% FCS and 10% tryptose-phosphate broth solution. The production of the recombinant RABV derived from the street strain 1088 and encoding the iRFP720 gene (1088/iRFP720) (Fig. 1A) was described previously (Isomura et al., 2017). The recombinant virus 1088/RFLuc (Fig. 1A) was generated in this study as described below.

2.3. Plasmid construction and generation of recombinant RABV 1088/RFLuc

The genome plasmid for the 1088 strain encoding the Red Firefly Luciferase gene (1088/RFLuc) was generated as follows. The RFLuc gene with an AgeI site, the Kozak sequence at the 5′ end, and a PacI site at the 3′ end was amplified by polymerase chain reaction using pCMV-Red Firefly Luc vector (Thermo Fisher Scientific) as a template, and then cloned into a pT7Blue T vector (Novagen, Merck Millipore). After DNA sequence confirmation, the RFLuc gene was subcloned into the reporter gene expression cassette of the genome plasmid of the recombinant 1088 strain in a swap using the AgeI and PacI sites (Isomura et al., 2017), resulting in the genome plasmid pCI-1088/RFLuc.

The recombinant 1088/RFLuc virus was generated and prepared as described previously (Isomura et al., 2017). pCI-1088/RFluc was transfected into BHK/T7-9 cells together with helper plasmids. The culture supernatant was collected after several days of incubation, and the recovered virus was amplified in SK-N-SH cells. Next, the virus was prepared in 10% (wt/vol) brain homogenate of suckling mice in phosphate-buffered saline (PBS) and stored in aliquots at −80 °C until use.

2.4. Virus titration

The infectious virus titer was determined in NA cells using a focus assay, as described previously (Yamada et al., 2012). The viral titer was expressed as focus forming units (FFU).

2.5. Evaluation of the antiviral activity of favipiravir against 1088/RFLuc in Neuro-2a cells

1088/RFLuc was inoculated into Neuro-2a cells on a 24-well plate at a multiplicity of infection (MOI) of 0.01. After virus adsorption for 1 h, the inoculum was removed and 1 mL of medium (MEM supplemented with 5% FCS and various concentrations of favipiravir) was added to each well. At 96 h postinoculation (hpi), the culture media were collected and infectious virus titers were determined using the focus assay. The cells were subjected to a luciferase assay to measure the relative light units per sec (RLU/sec) using a Pierce Firefly Luciferase Glow Assay Kit (Thermo Fisher Scientific) and a Gene Light GL-210 luminometer (Microtech, Chiba, Japan).

2.6. 6. In vivo imaging of mice infected with recombinant RABV

Six-week-old female hairless mice (Hos:HR-1) were purchased from Hoshino Laboratory Animals, Ibaraki, Japan. The mice were inoculated in the right hindlimb with 5×10^5 FFU of 1088/iRFP720 or 1088/RFLuc and then subjected to *in vivo* fluorescence or bioluminescence imaging, respectively. The fluorescence imaging was performed as described previously (Isomura et al., 2017). In brief, mice were imaged under inhalation anesthesia (2% isoflurane) using the Lumazone imaging system (Nippon Roper, Tokyo, Japan) equipped with an illumination system, an electron-multiplying (EM) charge-coupled device (CCD) camera, and fluorescence bandpass filters: 710/40 nm for excitation and 785/62 nm for emission. Imaging conditions were as follows: exposure time (EXP) of 400 msec and EM gain (EMG) of 10 (1–1,000). In addition, mice were fed a chlorophyll-free diet (D10001; Research Diets) from 1 week before virus inoculation. The bioluminescence imaging was conducted as follows. Mice were injected intraperitoneally (i.p.) with 150 mg/kg of D-luciferin potassium salt (Wako Pure Chemical Industries, Osaka, Japan) dissolved in PBS (0.2 mL) and imaged from 15 min after substrate administration under inhalation anesthesia (2% isoflurane) using the Lumazone imaging system with EXP of 2 min and EMG of 300. All images were acquired as 16-bit TIFF files and processed and analyzed using ImageJ software (Schneider et al., 2012).

2.7. Evaluation of the antiviral activity of favipiravir against RABV in mice using in vivo imaging

Six-week-old female hairless mice were inoculated intramuscularly (right hindlimb) with 10^5 FFU of 1088/RFLuc. Then, inoculated mice were administered favipiravir (300, 600, or 900 mg/kg/day) daily for

6–7 days, with administration commencing 1 hpi or 2 days post-inoculation (dpi). These treatments were administered twice daily (in the morning and in the afternoon) by oral gavage (20 mL/kg) under isoflurane anesthesia, with a 6-h interval in between doses. Mice were subjected to bioluminescence imaging as described above.

2.8. Animal ethics

All animal experiments were approved by the Animal Experiment Committee of Oita University (approval nos. 1610001 and 171001). All mice were humanely euthanized when they showed severe neurological signs.

2.9. Statistical analyses

Tukey's multiple comparisons test and the calculation of the half-maximal inhibitory concentration (IC_{50}) of favipiravir against 1088/RFLuc were performed using GraphPad Prism (version 6.0).

3. Results

3.1. 1. Establishing a highly sensitive in vivo imaging system for RABV infection

First, we compared the performance of the bioluminescence and fluorescence imaging systems for monitoring RABV infection using 1088/RFLuc and 1088/iRFP720 (Fig. 1A). Since animal fur is known to interfere with *in vivo* imaging analysis, we used the hairless mice strain Hos:HR-1, which is immunocompetent and has been shown to be suitable for *in vivo* imaging analysis (Schaffer et al., 2010; Suzuki et al., 2013). In addition, mice were inoculated in the right hindlimb with 5×10^5 FFU of each virus, as described in our previous study (Isomura et al., 2017). Bioluminescence imaging was performed longitudinally in the 1088/RFLuc-infected mice (Fig. 1B), and a bioluminescent signal was detected from the right hindlimb (the site of inoculation) at 1 dpi in two of four mice. At 3 dpi, bioluminescence was clearly observed from the right hindlimb in three mice, and a faint signal was also detectable in these mice at the lower end of the spinal cord. At 5 dpi, all mice showed a clear signal in the spinal cord, and a spot signal was detected in the brain of one mouse. From 6 to 8 dpi, the signal in the brain increased as time progressed, while also spreading through the whole body. No clinical signs of infection were observed until 6 dpi, but mice showed significant weight loss from 7 dpi and neurological symptoms from 7 to 8 dpi. In contrast, no obvious fluorescent signal was detectable until 5 dpi in mice inoculated with 1088/iRFP720. The signal began to be detected in the spinal cord at 6 dpi and in the brain from 7 dpi, coincident with the mice showing clinical signs of infection. Unlike the signal for bioluminescence, the fluorescent signal in other regions was weak or absent.

Overall, these findings indicated that the bioluminescence imaging system using 1088/RFLuc was a more sensitive method than fluorescence imaging for monitoring RABV infection dynamics.

3.2. The RFLuc reporter is sufficiently reliable to evaluate antiviral compounds

Next, we validated whether the RFLuc reporter gene of the recombinant virus could be used to accurately evaluate the antiviral activity of a compound using a cell culture system. Using a previously described protocol (Yamada et al., 2016), Neuro-2a cells were inoculated with 1088/RFLuc, and were then incubated with several concentrations of favipiravir for 96 h, after which both the infectious virus titer in the supernatant and the luciferase activity in the cells were determined and compared. The inhibition-rate curves based on the virus titer and RLU were similar, and the IC_{50} values were also almost identical using both methods (Fig. 2). In addition, the growth activity of 1088/RFLuc was not affected compared with that observed for the WT virus in Neuro-2a cells (Fig. S1). Hence, the measurement of the RFLuc activity of the recombinant virus was considered to be a reliable method of evaluation of the activity of antiviral compounds.

3.3. Evaluation of favipiravir treatment in infected mice using in vivo bioluminescence imaging

Previously, we had hypothesized that favipiravir (300 mg/kg/day) was ineffective against viruses located within the CNS, but effective before neuroinvasion (Yamada et al., 2016). To test this hypothesis, we conducted bioluminescence imaging of 1088/RFLuc-infected mice treated with favipiravir. Hairless mice were inoculated in the right hindlimb with 10^5 FFU of 1088/RFLuc and administered favipiravir (300 mg/kg/day) by oral gavage for 7 days, commencing at 1 hpi (0–6 dpi) or 2 dpi (2–8 dpi), as described in our previous report (Yamada et al., 2016). We confirmed that the pathogenicity of 1088/RFLuc was not affected compared with that observed in the WT virus at this challenge dose (Fig. S2). Fig. 3 shows that bioluminescence intensities at the spinal cord and brain were strongly suppressed in the infected mice given an immediate (1 hpi) dose of favipiravir compared with infected mice that were not treated over the indicated period. The immediate dosage almost completely suppressed bioluminescence at the inoculation site at 1 dpi (Fig. S3A). In contrast, in infected mice given the delayed treatment (2 dpi), the signal intensities at the spinal cord and brain were slightly but not significantly reduced compared with those in untreated infected mice. Hence, the bioluminescence imaging analysis supported our hypothesis that favipiravir (300 mg/kg/day) is ineffective against RABV located within the CNS. In addition, a survival analysis showed that the immediate dosage prolonged the survival time significantly, but did not improve the survival rate (Fig. S3B).

3.4. In vivo bioluminescence imaging revealed that higher dosage of favipiravir improved the antiviral effect in infected mice given delayed treatment

Increasing the dose of a compound is one simple way to improve treatment efficacy, and a dosage of 600 mg/kg/day favipiravir has been trialed to assess its efficacy against norovirus infection in a mouse model (Arias et al., 2014). We used bioluminescence imaging to evaluate the efficacy of higher doses of favipiravir (600 and 900 mg/kg/day) in the delayed-treatment model. Hairless mice were inoculated with 1088/RFLuc in the right hindlimb and orally administered favipiravir (300, 600, or 900 mg/kg/day) for 7 days commencing at 2 dpi. However, because the mice given the dose of 900 mg/kg/day gradually lost weight, they were treated for only 6 days (2–7 dpi). A summary of the results is shown in Fig. 4. Bioluminescence signals at the spinal cord and brain were reduced in a dose-dependent manner in the groups of infected mice treated with higher doses of favipiravir, and a significant reduction was observed in the mice given 900 mg/kg/day. However, higher dosages did not improve the survival time or rate significantly (Fig. S4). The mice that received a dose of 900 mg/kg/day died or were euthanized because of severe weight loss accompanied by the side effects. In addition, one of the untreated infected mice showed slow progression of the disease, with clinical signs being observed only from 12 dpi; this mouse was euthanized at 15 dpi (Fig. S4).

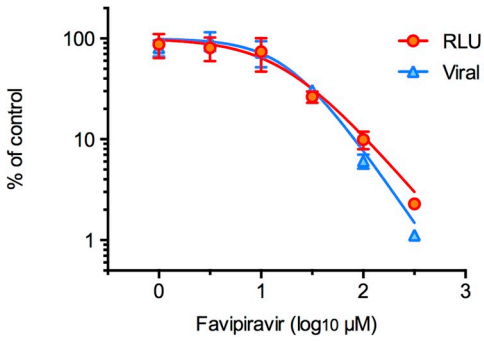

	IC50 (μM)	95% CI (μM)
RLU	16.34	10.10 - 26.43
Viral titer	18.39	12.69 - 26.66

Fig. 2. Antiviral activity of favipiravir against 1088/RFLuc in Neuro-2a cells. The cells were inoculated with 1088/RFLuc at an MOI of 0.01 and incubated for 96 h with the indicated concentration of favipiravir. The virus titer in each supernatant was determined using the focus assay, and the cells were lysed and subjected to a luciferase assay to determine RLU. The data represent the mean (n = 3) and standard deviation. A sigmoidal dose response was fitted using GraphPad Prism software. Mean values obtained from control wells (favipiravir 0 μM) were set as 100%. Each IC50 value with its 95% confidence interval (CI) is indicated.

4. Discussion

Because real-time visualization of viral replication dynamics in a small animal model is clearly useful for studies of virus infection, we previously established *in vivo* fluorescence imaging of RABV infection (Isomura et al., 2017). Although this system is very easy to use (e.g., no substrate is required and exposure time is under 1 s) to monitor virus replication dynamics in mice, it is limited in its ability to detect the early phase of infection. Because we expected that the system would have difficulty in dissecting how favipiravir acts on RABV in mice, we established the bioluminescence imaging system used in the present study. For this, we selected RFLuc as a reporter gene, because red-shifted light (> 600 nm) is favorable for deep-tissue imaging (Hong et al., 2017; Rice et al., 2001) and because its substrate, D-luciferin, can be administered i.p. NanoLuc, which is a brighter and smaller (19 kDa) luciferase derived from a deep-sea shrimp, was also a candidate because it has been used for the bioluminescence imaging of virus infections (Belarbi et al., 2019; Kanai et al., 2019; Karlsson et al., 2018; Sun et al., 2014; Tran et al., 2013). However, it emits blue light with a maximum emission at 460 nm (Hall et al., 2012), which is strongly absorbed and scattered in tissues (Hong et al., 2017; Rice et al., 2001), and its substrate, coelenterazine or its analog, is recommended to be administered intravenously. Therefore, we used 1088/RFLuc and succeeded in monitoring primary replication of RABV at the inoculation site from 1 dpi and its subsequent dissemination to the CNS, even though the imaging required an extended period (15 min of incubation after substrate injection and 2 min of exposure). Our previous immunohistochemical study demonstrated that at 3 dpi, viral antigen was detectable in the muscle of the inoculation site (the right hindlimb), but not in the lumbosacral dorsal root ganglion and spinal cord of mice infected with the 1088 strain (Kimitsuki et al., 2017). Thus, the bioluminescence imaging system established in this study has a sensitivity equivalent to or higher than that of the immunohistochemical detection, because faint bioluminescence was detected around the lower end of the spinal cord and at the inoculation site at 3 dpi (Fig. 1B). This highly sensitive imaging method is expected to be useful not only for evaluation of antiviral treatments but also for analysis of aspects of viral pathogenesis, such as attenuation, long incubation periods, and virus–host interactions.

The bioluminescence imaging of RABV infection in mice revealed that RABV also spread systemically concurrently with its ascension of the spinal cord to the brain, although it is believed that RABV centrifugally spreads from the CNS to the peripheral nerves/tissues at the end stage of infection (Begeman et al., 2018; Fisher et al., 2018). It is likely that our imaging system is sufficiently sensitive to detect the spread at an earlier phase of infection, which is difficult to detect with immunohistochemical methods because of the low level of viral antigen expression. Interestingly, bioluminescence signals thought to represent the centrifugal spread were detected as dots (e.g., as seen at 6 and 7 dpi in Fig. 1B). Our previous work showed that the 1088 strain prefers to replicate in the sensory nerve path in the spinal cord, rather than in the motor nerve path (Kimitsuki et al., 2017). Hence, it might be that we visualized the immediate spread of 1088/RFLuc to peripheral sensory nerves, some of whose terminals gathered at mechanoreceptors in the skin, at the sensory nerve-innervating sites in the spinal cord (Begeman et al., 2018; Owens and Lumpkin, 2014). However, even if so, it is also possible that viral proteins were trafficked more slowly to the terminal ends than the RFLuc protein and that therefore the centrifugal spread at the earlier phase has not been detected. Further analyses are needed to clarify these points.

Once we had confirmed using cultured cells that the bioluminescent reporter of 1088/RFLuc was sufficiently reliable to evaluate the antiviral efficacy of favipiravir, we evaluated the efficacy of treatment using bioluminescence imaging. We were able to demonstrate that favipiravir could suppress RABV replication at the site of inoculation but not after neuroinvasion, and therefore considered that an immediate postinoculation dose could reduce the viral load in the CNS (Fig. 3 and S3A). However, even the immediate dosage ultimately did not prevent lethal infection (Fig. S3B), indicating that favipiravir remains a limitation in the therapy for rabies. The BBB and BSCB are thought to interfere with the antiviral activity of favipiravir within the CNS. We found that increasing the dosages of favipiravir improved, although only partially, its antiviral activity in the CNS (Fig. 4). With higher doses, more favipiravir might be passively transported from the bloodstream into the CNS across these barriers, because favipiravir is a small molecule (MW: 157.1). However, because such an experimental trial is not practicable (we observed side effects in mice at a dosage of 900 mg/kg/day), we consider that enhancement of BBB permeability is required to increase the efficacy of favipiravir against RABV in the CNS and thereby is expected to cure symptomatic rabies. The enhancement of the BBB permeability is also important for RABV clearance from the CNS because it allows the entry of immune effectors, but pathogenic RABV strains do not cause the opening of the BBB during infection (Garcia et al., 2018; Hooper et al., 2009; Roy and Hooper, 2007, 2008; Roy et al., 2007). The combination therapy with antiviral drugs (including favipiravir) and mannitol, which causes opening of the BBB by osmotic disruption (Neuwelt et al., 1979), was tried but unable to cure rabies in a mouse model (Marosi et al., 2019; Martina et al., 2019; Smreczak et al., 2019). Our finding that infected mice started to show clinical signs when RABV had amplified strongly in the brain reinforces the reality that curing symptomatic rabies is highly challenging. Hence, for successful rabies treatment, it is necessary to find a highly effective system for drug delivery into the CNS. In addition, favipiravir is converted to its active form by the cellular enzyme, hypoxanthine-guanine phosphoribosyltransferase (HPRT), but the conversion rate of favipiravir is very low compared with those of the authentic substrates, hypoxanthine and guanine (Naesens et al., 2013). Therefore, identifying a way to enhance this conversion might also be promising.

There is no doubt that *in vivo* bioluminescence imaging is a powerful tool for evaluating the efficacy of antiviral interventions in rabies. Our

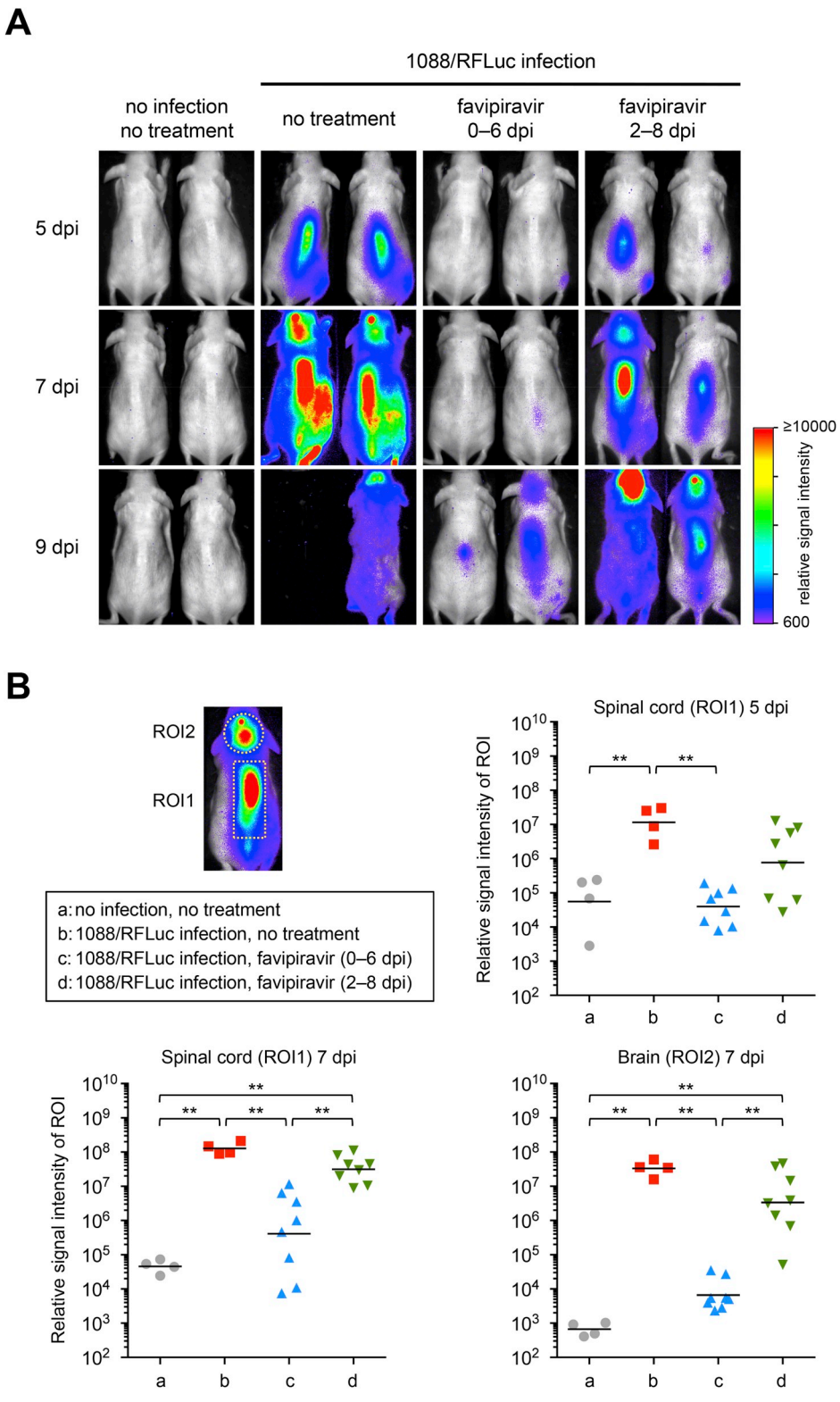

Fig. 3. *In vivo* bioluminescence imaging of 1088/RFLuc-infected mice treated with favipiravir. (A) Groups of eight hairless mice were inoculated with 1088/RFLuc (10^5 FFU) in the right hindlimb muscle and orally administered favipiravir (300 mg/kg/day) daily for 7 days, beginning 1 hpi (0–6 dpi) or 2 dpi (2–8 dpi). Uninfected control mice (n = 4) and infected mice without treatment (n = 4) were also included. Bioluminescence images were obtained as described in Fig. 1. Representative images of two mice in each group are shown. One of four infected mice without treatment was euthanized at 8 dpi. (B) Quantitative analysis of bioluminescence images. Regions of interest (ROIs) were set at the spinal cord (ROI1) and brain (ROI2) regions in the images as shown, and the relative signal intensities within the regions at the indicated time points were measured and plotted. Bars indicate geometric means. *P* values were determined using Tukey's multiple comparison test, and significant differences are shown (*$P < 0.05$, **$P < 0.01$).

findings show that the imaging system enabled us to better understand where and how the drug worked in RABV-infected mice. Moreover, the imaging system is a more humane method: the number of animals used in experiments can be reduced because semiquantitative data about viral load can be obtained longitudinally from the same animals; furthermore, our results showed that the imaging system enabled the evaluation of the anti-RABV efficacy in mice without necessarily recording the survival time and rate; this suggests that the duration of animal suffering and the experimental costs (time and effort) can be reduced. Finally, we consent to the recently proposed concept that an optimized combination therapy with virus-directed drugs (including their enhancers) and host-directed drugs (immune modulators and the BBB openers, etc.) is required for the effective treatment of symptomatic rabies (Marosi et al., 2019; Martina et al., 2019; Smreczak et al., 2019). *In vivo* bioluminescence imaging will be useful to facilitate the development of such treatment.

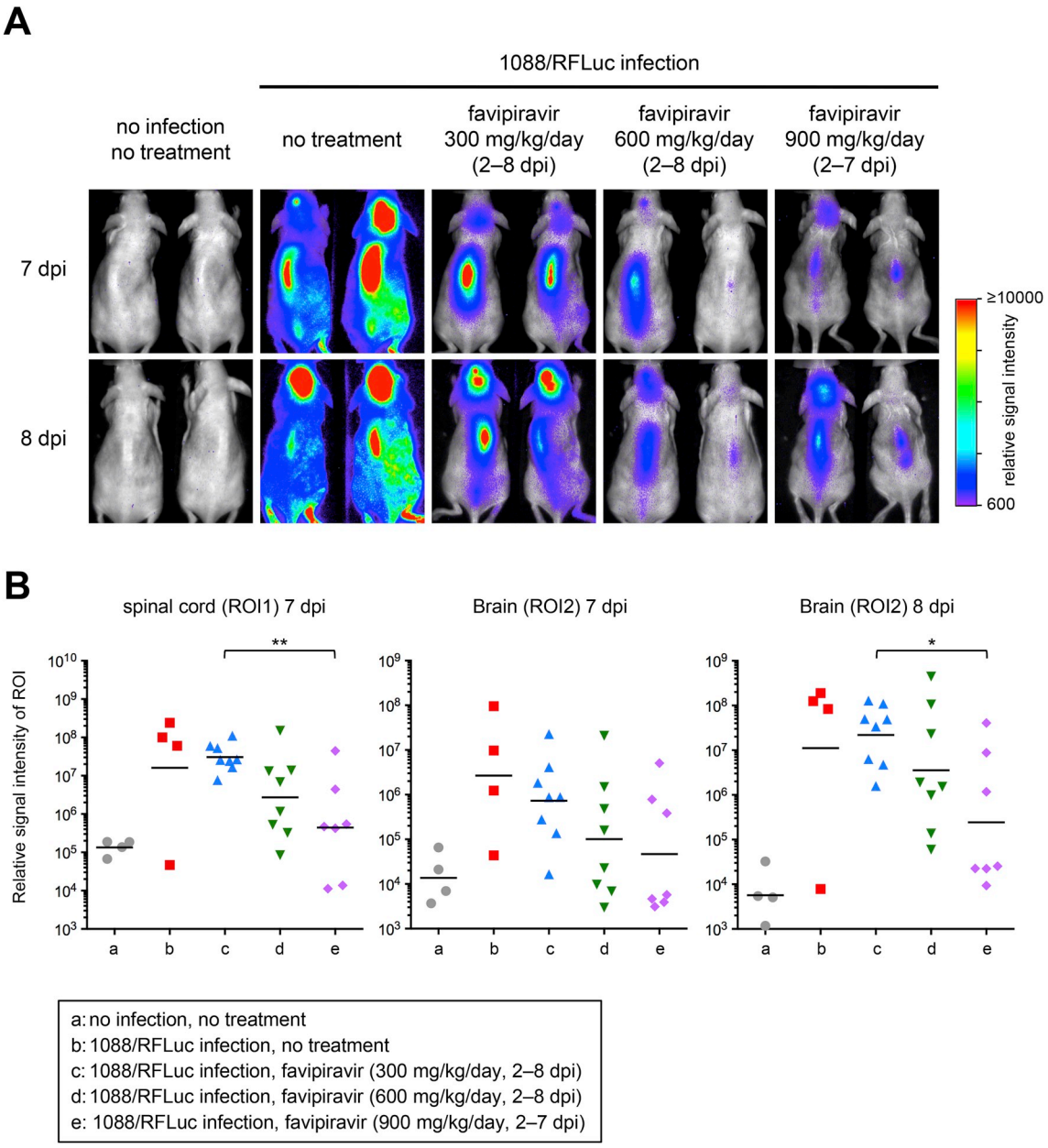

Fig. 4. Monitoring and analysis of higher-dose favipiravir treatment in infected mice. (A) Groups of seven or eight hairless mice were inoculated with 1088/RFLuc (10^5 FFU) in the right hindlimb muscle and orally administered favipiravir (300, 600, or 900 mg/kg/day) daily for 6–7 days, beginning at 2 dpi. Uninfected control mice (n = 4) and infected mice without treatment (n = 4) were also included. Bioluminescence images were obtained as described in Fig. 1. Representative images of two mice in each group are shown. (B) ROIs were set at the spinal cord (ROI1) and brain (ROI2) regions in the images as shown in Fig. 3, and the relative signal intensities within the regions at the indicated time points were measured and plotted. Bars indicate geometric means. Tukey's multiple comparison test was conducted to compare the three treatment groups, and significant differences are shown (*$P < 0.05$, **$P < 0.01$).

Declaration of competing interest

T. Komeno, N. Nakajima, and Y. Furuta are employees of FUJIFILM Toyama Chemical Co., Ltd., which is the producer of favipiravir. A. Nishizono received the funding to perform this study from FUJIFILM Toyama Chemical Co., Ltd. K. Yamada, K. Noguchi, K. Kimitsuki, R. Kaimori, and N. Saito have no conflicts of interest.

Acknowledgements

We thank to Drs Naoto Ito and Makoto Sugiyama (Gifu University, Japan) for providing BHK/T7-9 cells and helper plasmids. We also thank Dr. Koichi Morita (Nagasaki University, Japan) for providing Neuro-2a and SK-N-SH cells. This study was funded by FUJIFILM Toyama Chemical Co., Ltd.

Appendix A. Supplementary data

Supplementary data to this article can be found online at https://doi.org/10.1016/j.antiviral.2019.104641.

References

Arias, A., Thorne, L., Goodfellow, I., 2014. Favipiravir elicits antiviral mutagenesis during virus replication in vivo. Elife 3 e03679.

Banyard, A.C., Mansfield, K.L., Wu, G., Selden, D., Thorne, L., Birch, C., Koraka, P., Osterhaus, A., Fooks, A.R., 2019. Re-evaluating the effect of Favipiravir treatment on rabies virus infection. Vaccine 37, 4686–4693.

Begeman, L., GeurtsvanKessel, C., Finke, S., Freuling, C.M., Koopmans, M., Muller, T., Ruigrok, T.J.H., Kuiken, T., 2018. Comparative pathogenesis of rabies in bats and carnivores, and implications for spillover to humans. Lancet Infect. Dis. 18,

e147–e159.
Belarbi, E., Legros, V., Basset, J., Despres, P., Roques, P., Choumet, V., 2019. Bioluminescent ross river virus allows live monitoring of acute and long-term alphaviral infection by in vivo imaging. Viruses 11, E584.
Dorsaz, S., Coste, A.T., Sanglard, D., 2017. Red-shifted firefly luciferase optimized for Candida albicans in vivo bioluminescence imaging. Front. Microbiol. 8, 1478.
Dufkova, L., Sirmarova, J., Salat, J., Honig, V., Palus, M., Ruzek, D., Fooks, A.R., Mansfield, K.L., Tordo, N., Jochmans, D., Neyts, J., Martina, B., Koraka, P., Osterhaus, A., 2019. Mannitol treatment is not effective in therapy of rabies virus infection in mice. Vaccine 37, 4710–4714.
Fisher, C.R., Streicker, D.G., Schnell, M.J., 2018. The spread and evolution of rabies virus: conquering new frontiers. Nat. Rev. Microbiol. 16, 241–255.
Fooks, A.R., Cliquet, F., Finke, S., Freuling, C., Hemachudha, T., Mani, R.S., Muller, T., Nadin-Davis, S., Picard-Meyer, E., Wilde, H., Banyard, A.C., 2017. Rabies. Nat Rev Dis Primers 3, 17091.
Fuentes, S., Arenas, D., Moore, M.M., Golding, H., Khurana, S., 2017. Development of bioluminescence imaging of respiratory syncytial virus (RSV) in virus-infected live mice and its use for evaluation of therapeutics and vaccines. Vaccine 35, 694–702.
Furuta, Y., Gowen, B.B., Takahashi, K., Shiraki, K., Smee, D.F., Barnard, D.L., 2013. Favipiravir (T-705), a novel viral RNA polymerase inhibitor. Antivir. Res. 100, 446–454.
Garcia, S.A., Lebrun, A., Kean, R.B., Craig Hooper, D., 2018. Clearance of attenuated rabies virus from brain tissues is required for long-term protection against CNS challenge with a pathogenic variant. J. Neurovirol. 24, 606–615.
Guo, Z., Zhong, X., Lin, L., Wu, S., Wang, T., Chen, Y., Zhai, X., Wang, Y., Wu, H., Tong, L., Han, Y., Pan, B., Peng, Y., Si, X., Zhang, F., Zhao, W., Zhong, Z., 2014. A 3C(pro)-dependent bioluminescence imaging assay for in vivo evaluation of anti-enterovirus 71 agents. Antivir. Res. 101, 82–92.
Hall, M.P., Unch, J., Binkowski, B.F., Valley, M.P., Butler, B.L., Wood, M.G., Otto, P., Zimmerman, K., Vidugiris, G., Machleidt, T., Robers, M.B., Benink, H.A., Eggers, C.T., Slater, M.R., Meisenheimer, P.L., Klaubert, D.H., Fan, F., Encell, L.P., Wood, K.V., 2012. Engineered luciferase reporter from a deep sea shrimp utilizing a novel imidazopyrazinone substrate. ACS Chem. Biol. 7, 1848–1857.
Hampson, K., Coudeville, L., Lembo, T., Sambo, M., Kieffer, A., Attlan, M., Barrat, J., Blanton, J.D., Briggs, D.J., Cleaveland, S., Costa, P., Freuling, C.M., Hiby, E., Knopf, L., Leanes, F., Meslin, F.X., Metlin, A., Miranda, M.E., Muller, T., Nel, L.H., Recuenco, S., Rupprecht, C.E., Schumacher, C., Taylor, L., Vigilato, M.A., Zinsstag, J., Dushoff, J., 2015. Estimating the global burden of endemic canine rabies. PLoS Neglected Trop. Dis. 9, e0003709.
Hong, G., Antaris, A.L., Dai, H., 2017. Near-infrared fluorophores for biomedical imaging. Nat. Biomed. Eng. 1, 0010.
Hooper, D.C., Phares, T.W., Fabis, M.J., Roy, A., 2009. The production of antibody by invading B cells is required for the clearance of rabies virus from the central nervous system. PLoS Neglected Trop. Dis. 3, e535.
Hwang, S., Wu, T.T., Tong, L.M., Kim, K.S., Martinez-Guzman, D., Colantonio, A.D., Uittenbogaart, C.H., Sun, R., 2008. Persistent gammaherpesvirus replication and dynamic interaction with the host in vivo. J. Virol. 82, 12498–12509.
Isomura, M., Yamada, K., Noguchi, K., Nishizono, A., 2017. Near-infrared fluorescent protein iRFP720 is optimal for in vivo fluorescence imaging of rabies virus infection. J. Gen. Virol. 98, 2689–2698.
Ito, N., Takayama-Ito, M., Yamada, K., Hosokawa, J., Sugiyama, M., Minamoto, N., 2003. Improved recovery of rabies virus from cloned cDNA using a vaccinia virus-free reverse genetics system. Microbiol. Immunol. 47, 613–617.
Kanai, Y., Kawagishi, T., Matsuura, Y., Kobayashi, T., 2019. In vivo live imaging of oncolytic mammalian orthoreovirus expressing NanoLuc luciferase in tumor xenograft mice. J. Virol. 93 e00401-00419.
Karlsson, E.A., Meliopoulos, V.A., Tran, V., Savage, C., Livingston, B., Schultz-Cherry, S., Mehle, A., 2018. Measuring influenza virus infection using bioluminescent reporter viruses for in vivo imaging and in vitro replication assays. Methods Mol. Biol. 1836, 431–459.
Kimitsuki, K., Yamada, K., Shiwa, N., Inoue, S., Nishizono, A., Park, C.H., 2017. Pathological lesions in the central nervous system and peripheral tissues of ddY mice with street rabies virus (1088 strain). J. Vet. Med. Sci. 79, 970–978.
Koraka, P., Martina, B.E.E., Smreczak, M., Orlowska, A., Marzec, A., Trebas, P., Roose, J.M., Begeman, L., Gerhauser, I., Wohlsein, P., Baumgartner, W., Zmudzinski, J., Osterhaus, A.D.M.E., 2019. Inhibition of caspase-1 prolongs survival of mice infected with rabies virus. Vaccine 37, 4681–4685.
Luker, G.D., Bardill, J.P., Prior, J.L., Pica, C.M., Piwnica-Worms, D., Leib, D.A., 2002. Noninvasive bioluminescence imaging of herpes simplex virus type 1 infection and therapy in living mice. J. Virol. 76, 12149–12161.
Marosi, A., Dufkova, L., Forro, B., Felde, O., Erdelyi, K., Sirmarova, J., Palus, M., Honig, V., Salat, J., Tikos, R., Gyuranecz, M., Ruzek, D., Martina, B., Koraka, P., Osterhaus, A., Bakonyi, T., 2019. Combination therapy of rabies-infected mice with inhibitors of pro-inflammatory host response, antiviral compounds and human rabies immunoglobulin. Vaccine 37, 4724–4735.
Martina, B.E.E., Smreczak, M., Orlowska, A., Marzec, A., Trebas, P., Roose, J.M., Zmudzinski, J., Gerhauser, I., Wohlsein, P., Baumgartner, W., Osterhaus, A., Koraka, P., 2019. Combination drug treatment prolongs survival of experimentally infected mice with silver-haired bat rabies virus. Vaccine 37, 4736–4742.
McLatchie, A.P., Burrell-Saward, H., Myburgh, E., Lewis, M.D., Ward, T.H., Mottram, J.C., Croft, S.L., Kelly, J.M., Taylor, M.C., 2013. Highly sensitive in vivo imaging of Trypanosoma brucei expressing "red-shifted" luciferase. PLoS Neglected Trop. Dis. 7 e2571.
Mechlia, M.B., Belaid, A., Castel, G., Jallet, C., Mansfield, K.L., Fooks, A.R., Hani, K., Tordo, N., 2019. Dermaseptins as potential antirabies compounds. Vaccine 37, 4694–4700.
Mehle, A., 2015. Fiat Luc: bioluminescence imaging reveals in vivo viral replication dynamics. PLoS Pathog. 11, e1005081.
Mifune, K., Makino, Y., Mannen, K., 1979. Susceptibility of various cell lines to rabies virus. Japan J. Trop. Med. Hyg. 7, 201–208.
Naesens, L., Guddat, L.W., Keough, D.T., van Kuilenburg, A.B., Meijer, J., Vande Voorde, J., Balzarini, J., 2013. Role of human hypoxanthine guanine phosphoribosyltransferase in activation of the antiviral agent T-705 (favipiravir). Mol. Pharmacol. 84, 615–629.
Neuwelt, E.A., Maravilla, K.R., Frenkel, E.P., Rapaport, S.I., Hill, S.A., Barnett, P.A., 1979. Osmotic blood-brain barrier disruption. Computerized tomographic monitoring of chemotherapeutic agent delivery. J. Clin. Investig. 64, 684–688.
Owens, D.M., Lumpkin, E.A., 2014. Diversification and specialization of touch receptors in skin. Cold Spring Harb. Perspect. Med. 4, a013656.
Rameix-Welti, M.A., Le Goffic, R., Herve, P.L., Sourimant, J., Remot, A., Riffault, S., Yu, Q., Galloux, M., Gault, E., Eleouet, J.F., 2014. Visualizing the replication of respiratory syncytial virus in cells and in living mice. Nat. Commun. 5, 5104.
Rice, B.W., Cable, M.D., Nelson, M.B., 2001. In vivo imaging of light-emitting probes. J. Biomed. Opt. 6, 432–440.
Rogee, S., Larrous, F., Jochmans, D., Ben-Khalifa, Y., Neyts, J., Bourhy, H., 2019. Pyrimethamine inhibits rabies virus replication in vitro. Antivir. Res. 161, 1–9.
Roy, A., Hooper, D.C., 2007. Lethal silver-haired bat rabies virus infection can be prevented by opening the blood-brain barrier. J. Virol. 81, 7993–7998.
Roy, A., Hooper, D.C., 2008. Immune evasion by rabies viruses through the maintenance of blood-brain barrier integrity. J. Neurovirol. 14, 401–411.
Roy, A., Phares, T.W., Koprowski, H., Hooper, D.C., 2007. Failure to open the blood-brain barrier and deliver immune effectors to central nervous system tissues leads to the lethal outcome of silver-haired bat rabies virus infection. J. Virol. 81, 1110–1118.
Schaffer, B.S., Grayson, M.H., Wortham, J.M., Kubicek, C.B., McCleish, A.T., Prajapati, S.I., Nelon, L.D., Brady, M.M., Jung, I., Hosoyama, T., Sarro, L.M., Hanes, M.A., Rubin, B.P., Michalek, J.E., Clifford, C.B., Infante, A.J., Keller, C., 2010. Immune competency of a hairless mouse strain for improved preclinical studies in genetically engineered mice. Mol. Cancer Ther. 9, 2354–2364.
Schneider, C.A., Rasband, W.S., Eliceiri, K.W., 2012. NIH Image to ImageJ: 25 years of image analysis. Nat. Methods 9, 671–675.
Shcherbakova, D.M., Verkhusha, V.V., 2013. Near-infrared fluorescent proteins for multicolor in vivo imaging. Nat. Methods 10, 751–754.
Smreczak, M., Orlowska, A., Marzec, A., Trebas, P., Kycko, A., Reichert, M., Koraka, P., Osterhaus, A., Zmudzinski, J.F., 2019. The effect of combined drugs therapy on the course of clinical rabies infection in a murine model. Vaccine 37, 4701–4709.
Sun, C., Gardner, C.L., Watson, A.M., Ryman, K.D., Klimstra, W.B., 2014. Stable, high-level expression of reporter proteins from improved alphavirus expression vectors to track replication and dissemination during encephalitic and arthritogenic disease. J. Virol. 88, 2035–2046.
Suzuki, O., Koura, M., Noguchi, Y., Uchio-Yamada, K., Matsuda, J., 2013. Zygosity determination in hairless mice by PCR based on Hr(hr) gene analysis. Exp. Anim. 62, 267–273.
Tran, V., Moser, L.A., Poole, D.S., Mehle, A., 2013. Highly sensitive real-time in vivo imaging of an influenza reporter virus reveals dynamics of replication and spread. J. Virol. 87, 13321–13329.
Tran, V., Poole, D.S., Jeffery, J.J., Sheahan, T.P., Creech, D., Yevtodiyenko, A., Peat, A.J., Francis, K.P., You, S., Mehle, A., 2015. Multi-modal imaging with a toolbox of influenza a reporter viruses. Viruses 7, 5319–5327.
Troy, T., Jekic-McMullen, D., Sambucetti, L., Rice, B., 2004. Quantitative comparison of the sensitivity of detection of fluorescent and bioluminescent reporters in animal models. Mol. Imaging 3, 9–23.
Virojanapirom, P., Lumlertdacha, B., Wipattanakitchareon, A., Hemachudha, T., 2016. T-705 as a potential therapeutic agent for rabies. J. Infect. Dis. 214, 502–503.
Yamada, K., Noguchi, K., Komeno, T., Furuta, Y., Nishizono, A., 2016. Efficacy of favipiravir (T-705) in rabies postexposure prophylaxis. J. Infect. Dis. 213, 1253–1261.
Yamada, K., Park, C.H., Noguchi, K., Kojima, D., Kubo, T., Komiya, N., Matsumoto, T., Mitui, M.T., Ahmed, K., Morimoto, K., Inoue, S., Nishizono, A., 2012. Serial passage of a street rabies virus in mouse neuroblastoma cells resulted in attenuation: potential role of the additional N-glycosylation of a viral glycoprotein in the reduced pathogenicity of street rabies virus. Virus Res. 165, 34–45.